ISSN 1063-7826, Semiconductors, 2020, Vol. 54, No. 6, pp. 641–649. © Pleiades Publishing, Ltd., 2020.
Russian Text © The Author(s), 2020, published in Fizika i Tekhnika Poluprovodnikov, 2020, Vol. 54, No. 6, pp. 533–541.

SEMICONDUCTOR STRUCTURES, LOW-DIMENSIONAL SYSTEMS, AND QUANTUM PHENOMENA

Electronic Properties of Silicene Films Subjected to Neutron Transmutation Doping

A. E. Galashev[a,b,*] and A. S. Vorob'ev[a]

[a] *Institute of High-Temperature Electrochemistry, Ural Branch, Russian Academy of Sciences, Yekaterinburg, 620990 Russia*
[b] *Ural Federal University, Yekaterinburg, 620002 Russia*
**e-mail: galashev@ihte.uran.ru*

Received September 2, 2019; revised January 28, 2020; accepted January 29, 2020

Abstract—The radiation doping of single-crystal silicon with phosphorus retains the structure of the sample, reduces internal stresses, and increases the lifetime of minority charge carriers. The study is concerned with the effect of phosphorus additives on the electronic properties of silicene. The electron density-of-states spectra of a phosphorus-doped single layer and 2 × 2 bilayer silicene on a graphite substrate are calculated by the quantum-mechanical method. The carbon substrate imparts semiconductor properties to silicene due to *p*–*p* hybridization. Doping with phosphorus can retain or modify the metal properties gained by silicene. The position of phosphorus dopant atoms in silicene influences the semiconductor–conductor transition. The theoretical specific capacity of a phosphorus-doped silicene electrode decreases, and the electrode becomes less efficient for application in lithium-ion batteries. However, the increase in the conductivity is favorable for use of this material in solar cells.

Keywords: graphite, silicene, phosphorus, electron states
DOI: 10.1134/S1063782620060068

1. INTRODUCTION

Development of the technology of fabricating silicon thin films has made it possible to produce thin-film transistors and flexible solar cells and to reduce their cost [1]. Silicon thin films are fabricated by several techniques, such as electrodeposition from molten salts onto metal or glassy carbon substrates [2, 3], chemical-vapor deposition (CVD) with the activation of precursors by different methods [4], and plasma-enhanced epitaxial growth on silicon wafers [5]. The thinnest silicon film is silicene, a two-dimensional (2D) material with a band gap of (BG) ~27 meV. Silicene has already been produced on Ag(111) [6, 7], ZrB_2(0001) [8], and Ir(111) [9] substrates. The deposition of silicene on graphite was demonstrated in [10]. It was suggested that silicene, as well as silicon thin films, be used in solar cells [11], microelectronic devices [12], and lithium-ion batteries [13]. The properties of silicene have been studied by means of quantum-mechanical simulation [14] and classical molecular dynamics [15, 16]. To increase the service life of solar cells and to impart *n*-type conductivity [17, 18], silicon thin films are subjected to neutron doping [19], during which silicon partially transforms into phosphorus in accordance with the reaction

$$Si^{30} + n \rightarrow Si^{31}(2.62h) \rightarrow P^{31} + \beta^{-}. \quad (1)$$

Here, *n* denotes a neutron, the letter "h" abbreviates the word "hour", and β^- refers to β radiation.

The neutron doping of semiconductors is performed to improve their electrical properties. If a nucleus absorbs a neutron, the resultant composite nucleus can be in an unstable state until it becomes stable. In this case, the atomic number of the element can change because of nuclear transmutation. The irradiation of Si with thermal neutrons induces only one nuclear reaction with a short half-life of ^{31}Si (2.62 h).

The ^{31}P atom contains five electrons in the outer shell. Therefore, as a result of such neutron transmutation doping (NTD), the semiconductor is doped with an *n*-type impurity. In the case of doping high-resistivity silicon, the NTD technique is the most precise and consistent method of introducing phosphorus. In this case, the key parameter is the resistivity, which is representative of the concentration of charge carriers. Irradiation makes it possible to attain uniform doping. In this case, the fluence (the integral of the neutron flux or energy density over time) defines the degree of doping. The levels of conductivity of degenerate or very heavily doped semiconductors are comparable to the corresponding levels of metals. As in metals, in degenerate semiconductors, the occupied and unoccupied energy levels are not separated by a band gap. Degenerate semiconductors are often used

as alternatives to metals in present-day integrated circuits. Identical samples produced by the NTD technique exhibit small differences between their resistivities. This is achieved by accurately monitoring the irradiation dose, by aging the samples after irradiation, and if necessary, by annealing for the removal of irradiation-induced defects.

The phosphorus concentration (cm^{-3}) in *n*-doped silicon is determined by the expression

$$[P] = 1/(\rho e \mu), \quad (2)$$

where ρ is the resistivity (Ω cm), *e* is the elementary charge, and μ is the electron drift mobility in the crystal lattice of silicon. Doping should be performed under accurate monitoring of the neutron flux. It is desirable that thermal neutrons are dominant in the irradiation spectrum to reduce radiation damage formed in the crystal lattice by fast neutrons.

The purpose of this study is to investigate the electronic properties of silicene on a carbon substrate after NTD, i.e., after the transformation of 6.25–25% of silicon atoms into phosphorus.

2. DESCRIPTION OF THE MODEL

Calculations of the electronic properties of modified silicene were carried out with the use of Siesta software [20]. In this study, we consider the results of the neutron irradiation of silicene on a carbon substrate. Upon such irradiation, some silicon atoms of silicene transform into phosphorus atoms. Silicene was represented in two ways, specifically, by a single-layer structure formed as a 2 × 2 supercell (eight silicon atoms located in two *xy* planes) and by a bilayer structure formed as two 2 × 2 silicene supercells (sixteen silicon atoms located in four *xy* planes). The calculations were performed for both self-supporting silicene and silicene on a carbon substrate. The thickness of the carbon substrate was chosen by carrying out an additional computer simulation. We considered substrates consisting of one to four graphite layers. One layer of the substrate was specified as consisting of 18 carbon atoms, i.e., forming a 3 × 3 supercell. All of the atoms of the silicene–(carbon substrate) system were subjected to geometric optimization. However, the transition from bulk layered material to a 2D structure consisting of only few layers is accompanied by a decrease in the interlayer spacing. Therefore, if the number of graphite layers in the model is larger than unity, the carbon atoms of each layer are fixed in the vertical direction. This approach allowed us to retain the interlayer spacing in the substrate at the experimentally established level 0.3314 nm in graphite.

Table 1. Energy of adhesion of silicene consisting of one and two sheets to a graphite substrate consisting of one to four layers (eV per unit cell)

Number of silicene sheets	Number of layers of the graphite substrate			
	1	2	3	4
1	0.122	0.131	0.133	0.132
2	0.124	0.092	0.094	0.091

In the calculations, we used the Born–Karman periodic boundary conditions involved in the Siesta software. The translation parameters for the graphene and silicene supercells were 0.741 and 0.774 nm, respectively. The translation parameter of the combined silicene–graphite supercell in the *x* and *y* directions was chosen to be 0.7575 nm equal to the corresponding parameter used in [21], wherein it was shown that the electronic properties of both self-supporting silicene and graphene in the combined supercell were

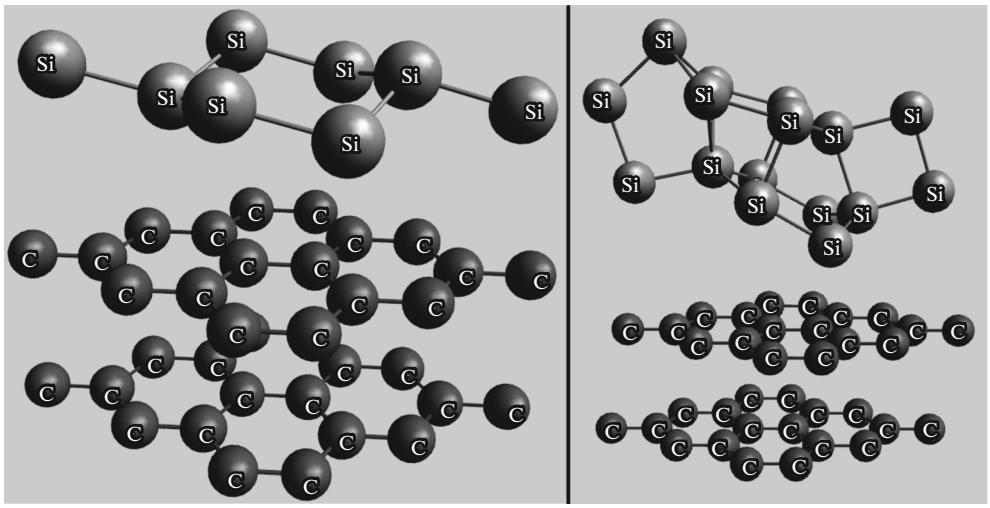

Fig. 1. Configuration of the Si–C systems after geometric optimization: (left) single layer and (right) bilayer silicene. A graphite substrate consisting of two layers is shown.

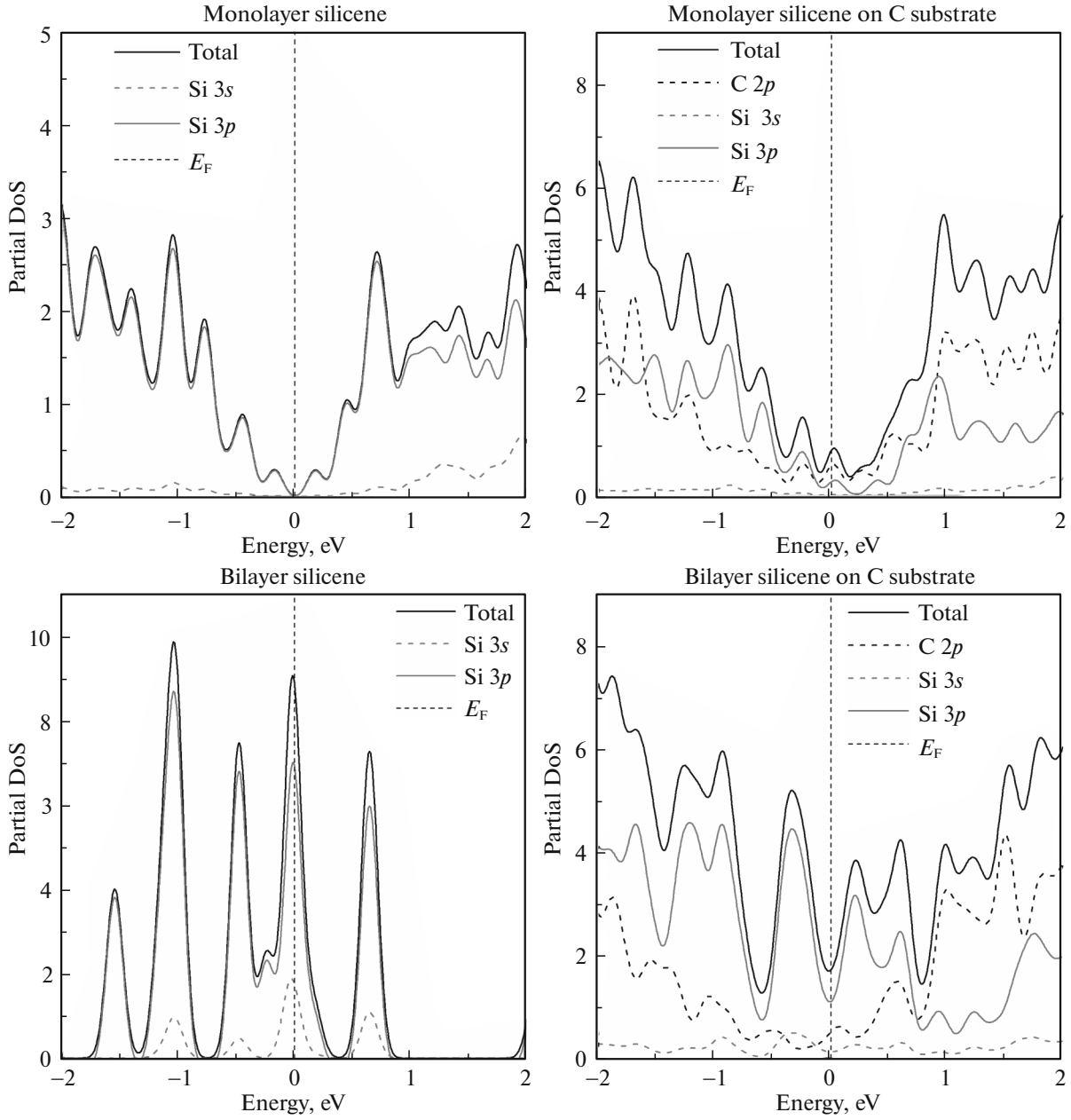

Fig. 2. Partial DoS spectra of single layer and bilayer silicene: (left) self-supporting silicene and (right) silicene on a graphite substrate.

retained. The value of the translation vector in the z direction was chosen to be 35 Å. Thus, the system was an infinitely translated short-period superlattice. Similar superlattices are often used for the simulation of 2D systems. For example, the 3×3 graphene supercell was used to determine the energy of adsorption of aluminum and silver [22] and to study the storage of hydrogen on graphene with adsorbed palladium [23]. The 2×2 silicene supercell served as a basic element for determining the limiting lithiation of silicene [24] and for establishing the possibility of storing hydrogen on metal-functionalized silicene [25].

Doping was conducted by replacing silicon atoms with phosphorus atoms. In the study of a silicene single layer and bilayer on a graphite substrate, replacement that represented NTD was performed for one or two silicon atoms. Such replacement was performed for atoms located in all possible positions of atoms in silicene, including its upper and lower sublattices. Then all of the characteristics calculated were averaged over the sets of configurations considered. The partial electron density-of-states (DoS) spectra were constructed. The systems were subjected to geometric optimization using the generalized gradient approxi-

Table 2. Geometric and energy characteristics of modified single layer and bilayer silicene without and with a carbon substrate

Property	Without a substrate				With a graphite substrate			
	one Si layer		two Si layers		one Si layer		two Si layers	
	1P	2P	1P	2P	1P	2P	1P	2P
Si–Si_{int}, Å	0.60	0.66	0.75	0.76	0.66	0.72	1.05	1.04
Δ_{Si}, Å	–	–	1.96	1.98	–	–	2.07	2.06
Si–Si_{bond}, Å	2.33	2.29	2.36	2.38	2.29	2.31	2.38	2.38
Si–P, Å	2.32	2.27	2.32	2.35	2.28	2.32	2.36	2.35
E_{ad}, eV (unit cell)$^{-1}$	–	–	–	–	0.130	0.128	0.085	0.086
E_{bond}, eV	4.72	4.72	4.94	4.95	4.815	4.836	5.020	5.051
C_{TS}, mA h g^{-1}	3980.7	3768.0	4089.1	3980.7	1616.3	1552.7	2272.2	2222.6
BG, eV	M	M	M	M/0.236	M	M	M	M/0.018/0.009

mation proposed by Perdew, Burke, and Ernzerhof (PBE). The dynamic relaxation of atoms was conducted until the change in the total energy of the system was smaller than 0.001 eV. The energy of cutoff of the basis of plane waves was taken to be 200 Ry. The Brillouin zone was specified by Monkhorst–Pack's method, using 10 × 10 × 1 k points. The study was based on the double-exponential (double-zeta) polarization (DZP) basis set.

The energy of adhesion of a perfect silicene sheet to a graphite substrate was calculated in accordance with the formula

$$E_{ad} = \frac{-(E_{tot} - E_{Si(P)} - E_C)}{n_{cell}}. \quad (3)$$

Here, E_{tot} is the total energy of the whole system, $E_{Si(P)}$ is the total energy of silicene (unirradiated or doped with phosphorus), E_C is the total energy of the carbon substrate, and n_{cell} is the number of unit cells in the silicene supercell. In this case, the phosphorus atoms in the system were considered as belonging to the silicene supercell.

The general expression for the bonding energy in silicene in the systems under consideration is

$$E_{bond} = \frac{-(E_{tot} - n_{Si}E_{Si} - n_P E_P - E_C)}{n}. \quad (4)$$

Here, E_{Si} and E_P are, correspondingly, the total energies calculated for one silicon and phosphorus atom; n_{Si} and n_P are the numbers of silicon and phosphorus atoms in the system, $n = n_{Si} + n_P + n_C$ is the number of all atoms in the system.

The theoretical specific capacity of the modified silicene sheet that plays the role of an electrode in a chemical current source was calculated by the formula

$$C_{TS} = \frac{x\mathrm{F}}{M}. \quad (5)$$

Here, x is the number of interacting electrons, F is the Faraday number, and M is the molar mass of elements in the system.

3. RESULTS AND DISCUSSION

We calculated the physical parameters of both self-supporting (substrate-free) single layer and bilayer silicene (Si) and silicene on a graphite substrate (Si–C). To determine the optimal number of layers of the substrate, we considered four systems containing 1–4 graphene layers consisting of 18–72 carbon atoms. After geometrical optimization of these systems, we calculated the adhesion energies E_{ad} that describe the bonding between silicene and the carbon substrate. Table 1 lists the adhesion energies in relation to the number of layers in the graphite substrate. It can be seen that an increase in the substrate thickness from two to three layers is accompanied by a change in the adhesion energy by ~1.5% in both cases of single layer and bilayer silicene. Taking into account the four layers of the substrate results in a no larger than 1.1% difference in E_{ad} from the variant of two layers for both cases. Therefore, in further calculations, we considered a graphite substrate consisting of two layers containing 36 carbon atoms.

Figure 1 schematically shows the Si–C systems after geometric optimization. Upon optimization, the systems undergo noticeable geometric transformations relative to the atomic arrangement in self-supporting unmodified silicene. Specifically, the average spacing between silicene sublattices Si–Si_{int} increases from 0.44 to 0.56 Å and from 0.44 to 1.01 Å for single layer and bilayer silicene, respectively.

The partial DoS spectra of self-supporting single layer and bilayer silicene and silicene on a carbon substrate are shown in Fig. 2. Single-layer silicene is a semiconductor with a band gap of 0.027 eV. The arrangement of silicene on a graphite substrate brings

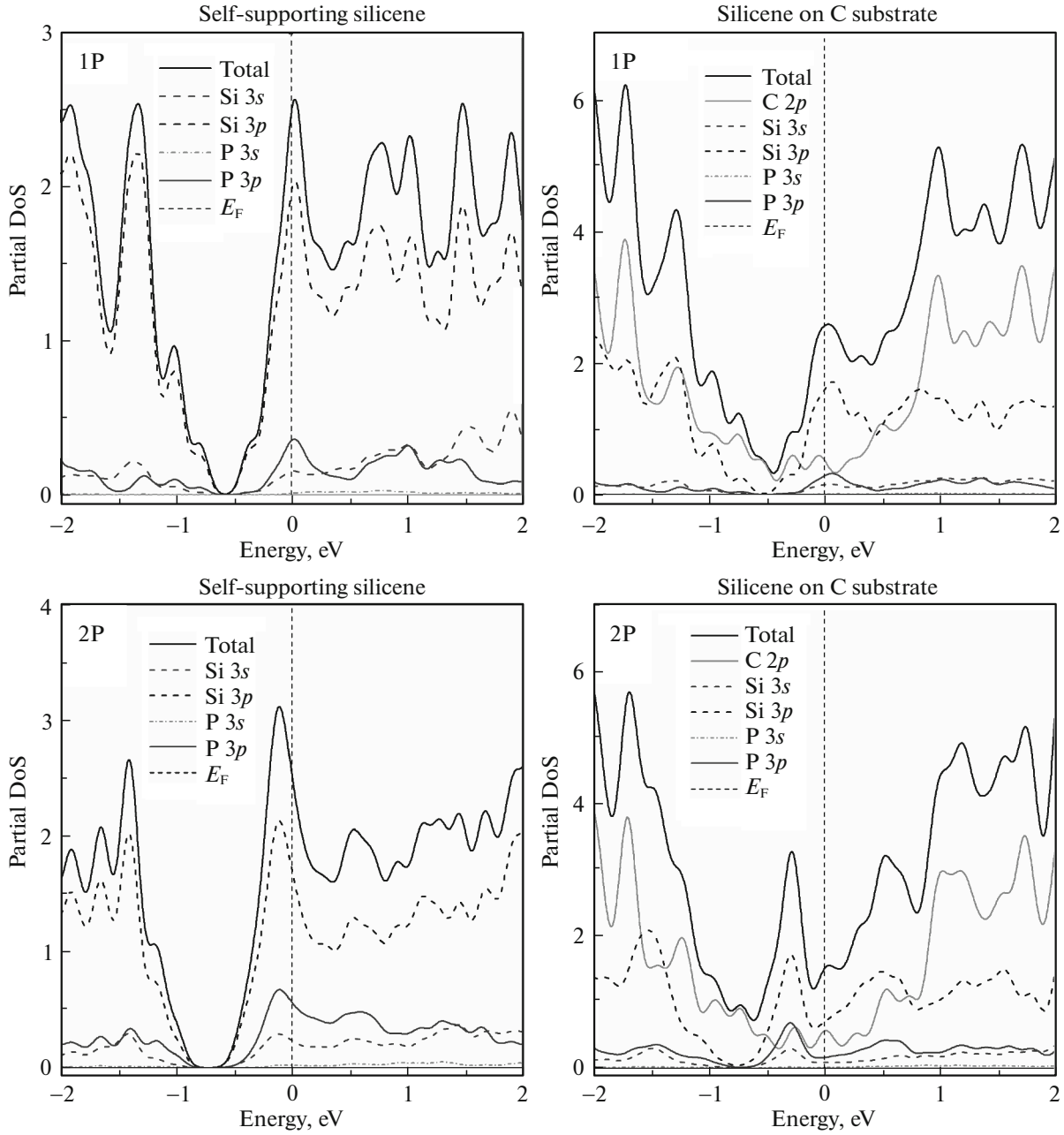

Fig. 3. Partial electron DoS spectra of single-layer silicene upon the substitution of phosphorus atoms for one and two silicon atoms: (left) self-supporting modified single-layer silicene and (right) similar silicene on a graphite substrate.

about the appearance of semiconductor properties. The electron conduction in single-layer silicene is a consequence of its interaction with the substrate. As can be seen from Fig. 2, the conduction is a result of the interaction of 2*p* electrons of carbon with 3*p* electrons of silicene, which is consistent with the data reported in [26, 27]. The calculations performed here show that bilayer silicene is a conductor due to the interaction of *p* and *s* electrons of its different layers. The appearance of metal conduction in bilayer silicene was shown also in [28].

The number of silicon atoms replaced by phosphorus was varied from one to two in all cases under consideration. Table 2 gives the calculated characteristics, such as the average spacings between silicene sublattices (Si–Si_{int}), the average spacing between silicene sheets (Δ_{Si}), the average lengths of bonds between silicon atoms (Si–Si_{bond}) and between silicon and phosphorus atoms (Si–P), the energy of the adsorption of phosphorus-modified silicene on a carbon substrate (E_{ad}), the bonding energy in phosphorus-modified silicene (E_{bond}), the theoretical specific capacity of the

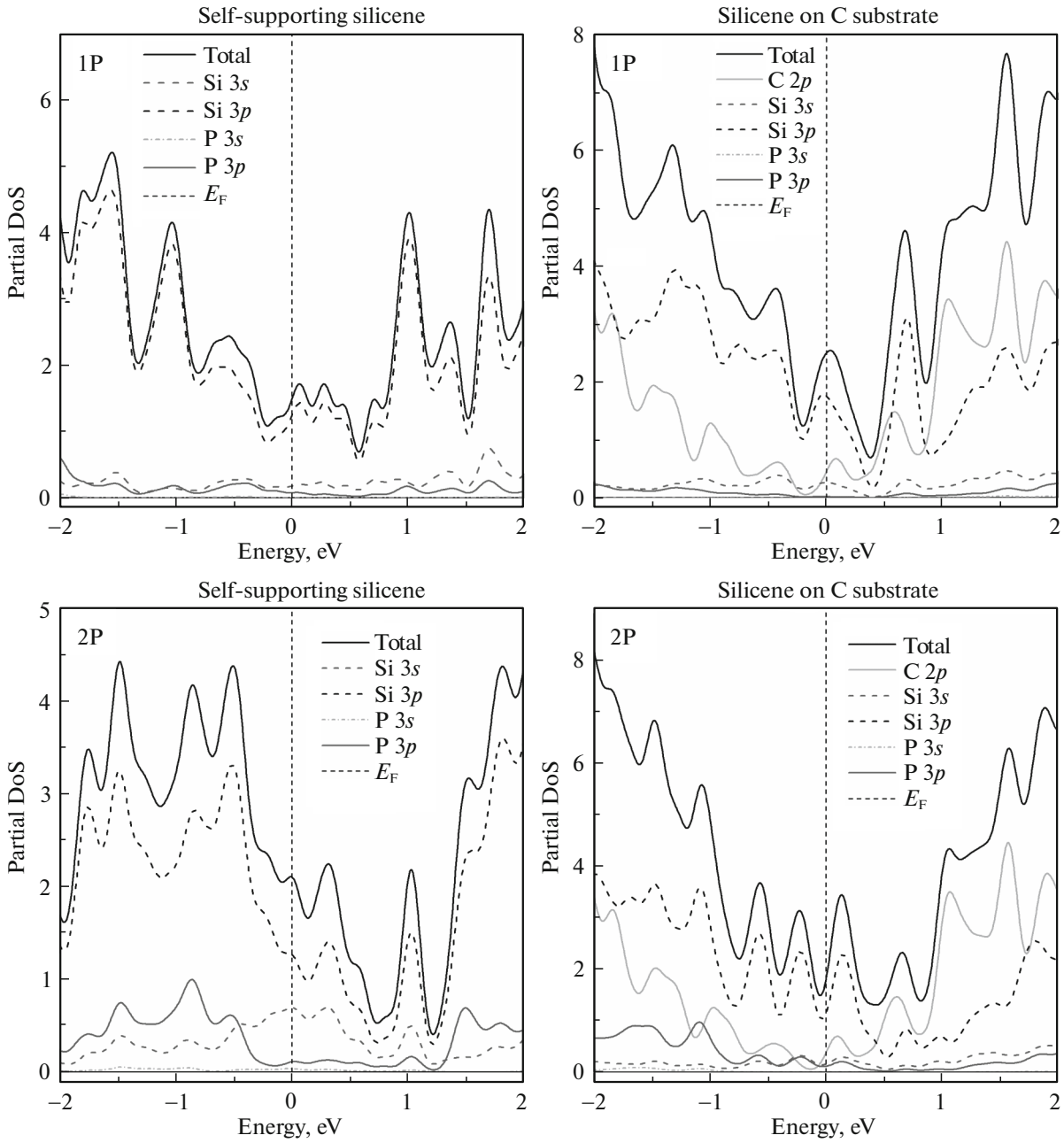

Fig. 4. Partial electron DoS spectra of bilayer silicene upon the substitution of phosphorus atoms for one and two silicon atoms: (left) self-supporting modified bilayer silicene and (right) similar silicene on a graphite substrate.

systems under consideration (C_{TS}), and the band gap. As the number of silicon atoms replaced by phosphorus in silicene is increased, the spacing between sublattices Si–Si_{int} increases from 0.44 to 0.66 Å. For silicene on a graphite substrate, the Si–Si_{bond} and Si–P bond lengths correspond to the same characteristics of self-supporting silicene, ≈2.31 Å.

The interplanar spacing between the carbon substrate and the lower sublattice of silicene, Si–C_{int}, is ~3.44 Å in all cases under consideration. The average Si–C_{bond} and C–C bond lengths are found to be also independent of the number of phosphorus atoms and equal to 3.64 and 1.44 Å, respectively. The spacing between silicon atoms (Si–Si_{bond}) is close to 2.31 Å in the phosphorus-modified self-supporting silicene sheet and the corresponding silicene layer on the carbon substrate. However, in bilayer silicene in both cases, the Si–Si bond length is larger and reaches 2.38 Å. An increase in the Si–Si_{bond} bond lengths results from an increase in the spacing between the sublattices of silicene. In the presence of a graphite

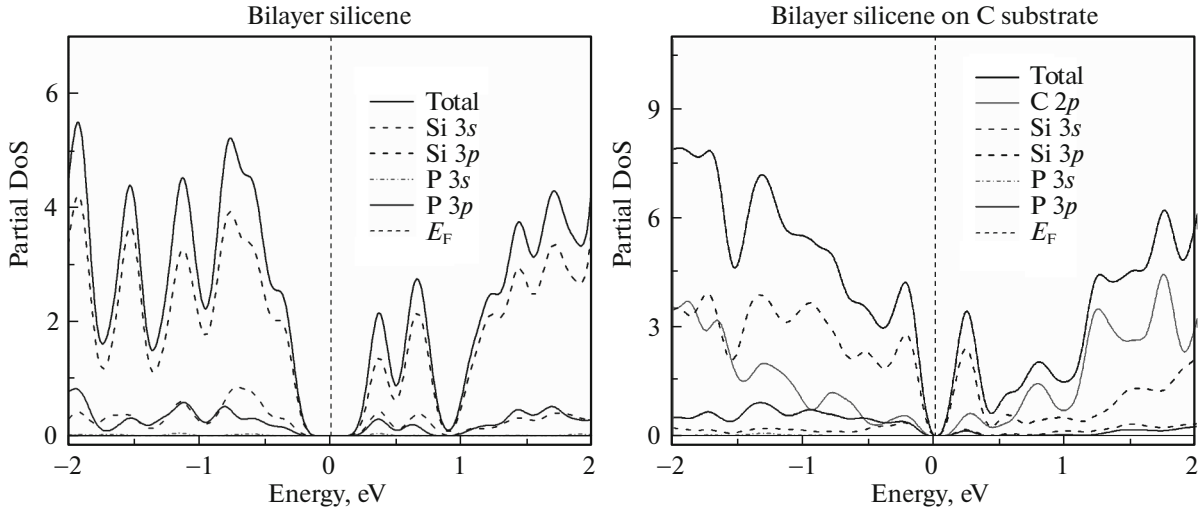

Fig. 5. Partial electron DoS spectra of bilayer silicene after replacement of a silicon atom by a phosphorus atom in the lower sublattice of each of the silicene sheet: (left) self-supporting silicene and (right) silicene on a graphite substrate.

substrate, the spacing between sheets of both unmodified and modified bilayer silicene Δ_{Si} increases by ~5%. In this case, it is found that there is no dependence of Δ_{Si} on the number of phosphorus atoms in silicene. The substrate and the number of phosphorus atoms ambiguously influence the Si–P bond length. The shortest Si–P bond length (2.28 Å) is obtained for single-layer silicene on a substrate. This length is close to the Si–P bond length (2.24 Å) determined in the ab initio study of the chemical functionalization of silicene with phosphorus [29]. The Si–Si_{bond} lengths are larger than the Si–P bond length by 1–2%. The Si–Si_{bond} and Si–P bond lengths obtained here are in agreement with the data reported in [30, 31].

The substitution of phosphorus for silicon influences also the energy characteristics of the system (Table 2). The relative bond energy E_{bond} in a single layer and bilayer of self-supporting silicene containing one phosphorus atom is 4.72 and 4.94 eV, respectively. As one more silicon atom is replaced by a phosphorus atom, the bond energy in single-layer silicene remains unchanged, whereas the bond energy in bilayer silicene increases to 4.95 eV. In the presence of the carbon substrate, the bond energy increases in both single-layer and bilayer silicene regardless of how many silicon atoms are replaced by phosphorus atoms.

The energy of adhesion of single-layer silicene doped with one phosphorus atom to the graphite substrate is ~35% higher than the energy of adhesion of bilayer silicene with the same composition to the same substrate. In general, this situation holds after the doping of silicene with two phosphorus atoms; in this case, the difference between the adhesion energies for single layer and bilayer silicene is 33%. In Table 2, the letter M in the row BG denotes "metal", and the figures in the row BG indicate the band gap (in eV) that can appear in a particular configuration.

The possibility of using the nanocomposites under study in solar-power engineering and as the anode of lithium-ion batteries is verified by estimating the available high specific capacity C_{TS}. To estimate the gravimetric capacity, we used relations corresponding to maximum lithiation of the constituent materials of the electrode: $SiLi_{4.4}$ [32], PLi_3 [33], and C_6Li [34]. Anodes based on silicon possess a theoretical capacity $C_{TS} = 4200$ mA h g^{-1} that can be attributed to a self-supporting single layer and bilayer silicene as well. The limiting capacity of perfect silicene on a graphite substrate decreases to 2322.2 mA h g^{-1} for single-layer silicene and to 2955.7 mA h g^{-1} for bilayer silicene. It should be noted that, as silicon is partially replaced by phosphorus, the theoretical specific capacity C_{TS} decreases because of the large mass of phosphorus and a decrease in the theoretical maximum number of electrons involved in the reaction with lithium (from 4.4 electrons for silicon to 3 electrons for phosphorus). Thus, the capacity C_{TS} calculated for a self-supporting modified silicene sheet is larger than the corresponding value for the (modified silicene)–(carbon substrate) system.

The doping of single-layer silicene with phosphorus, as well as the arrangement of such silicene on a graphite substrate, results in metallization of the system. The partial electron DoS spectra of the phosphorus-modified self-supporting silicene sheet and the corresponding single-layer silicene on a carbon substrate are exemplified in Fig. 3. The introduction of phosphorus atoms into silicene brings about the appearance of conduction, since phosphorus is an element with five outer electrons, whereas silicon possesses only four outer electrons. In other words, the

incorporation of a phosphorus atom into the silicene structure is bound to give one free electron. As even one phosphorus atom is introduced into the silicene sheet, the energy gap between the valence band and conduction band disappears, and silicene takes on conductor properties because of p–p hybridization, which is in agreement with the data of [29]. A further increase in the number of replaced silicon atoms to two does not change the conductor properties of the system (Fig. 4).

Figure 4 shows the partial spectra of the most probable electron states of phosphorus-modified bilayer silicene. Both self-supporting bilayer silicene and similar silicene on a carbon substrate, as a rule, retain their conductor properties. However, in a special case where silicon atoms replaced with phosphorus atoms are located in the lower sublattice of the upper or lower silicene sheet, the system subjected to doping can take on semiconductor properties.

The spectra of electron states for one such variant of doping (phosphorus atoms are located in the lower sublattices of the upper and lower silicene sheets) are shown in Fig. 5. It can be seen that, in self-supporting silicene in this case, the system transforms into the semiconductor state with the band gap 0.236 eV. In the presence of a graphite substrate, the band gap of bilayer silicene in the above-indicated configuration narrows to 0.018 eV. A similar transition to the semiconductor state was observed upon the substitution of phosphorus atoms for two silicon atoms in the lower sublattice of the lower silicene sheet. In such a case, self-supporting bilayer silicene is metallized, whereas silicene on a carbon substrate takes on semiconductor properties with the band gap ~0.009 eV.

4. CONCLUSIONS

The results obtained in the study show that, at a content of phosphorus from 6 to 25% in self-supporting modified single layer and bilayer silicene, the system is metallized because of the interaction of 3p electrons of silicon with 3p electrons of phosphorus. A successive increase in the content of phosphorus in silicene yields a gradual increase in the spacing between the sublattices of silicene. The substitution of phosphorus atoms for silicon atoms in the silicene–(graphite substrate) system makes the system more stable, which is due to geometric rearrangements in the silicene sheet. In bilayer silicene, the Si–Si bond length is 3% larger than that in the single-layer silicene sheet. Elongation of the bond correlates with an increase in the spacing between the sublattices of silicene. Shortening of the Si–P bond length by 1–2% compared to the Si–Si bond length does not result in any substantial transformation of the crystal structure of silicene.

As a result of p–p hybridization, the silicene–(carbon substrate) system takes on semiconductor properties in most cases. However, the presence of two phosphorus atoms replacing silicon atoms in bilayer silicene makes possible the conductor–semiconductor transition. This transition is associated with a certain position of these atoms in bilayer silicene.

Thus, to improve the semiconductor properties of silicene on a carbon substrate, it is necessary not only to choose the appropriate neutron irradiation fluence that determines the number of transmutations of silicon to phosphorus, but also to know the neutron energy in order to control the formation of defects and the geometric parameters of the nanocomposite. The control of doping with phosphorus will aid in fabricating a final product with a specified uniform resistivity. This can be attained with a rather homogeneous structure of modified silicene.

FUNDING

The study was supported by the Russian Science Foundation, project no. 16-13-00061.

CONFLICT OF INTEREST

The authors declare that they have no conflict of interest.

REFERENCES

1. A. G. Aberle, Thin Solid Films **517**, 4706 (2009).
2. A. V. Isakov, A. P. Apisarov, A. O. Khudorozhkova, M. V. Laptev, and Yu. P. Zaikov, J. Phys.: Conf. Ser. **1134**, 012021 (2018).
3. S. I. Zhuk, L. M. Minchenko, O. V. Chemezov, V. B. Malkov, O. V. Grishenkova, V. A. Isaev, Yu. P. Zaikov, and Sh. Qi, Adv. Mater. Res. **1088**, 429 (2015).
4. M. N. Andreev, A. K. Rebrov, A. I. Safonov, N. I. Timoshenko, K. V. Kubrak, and V. S. Sulyaeva, J. Eng. Phys. Thermophys. **88**, 1003 (2015).
5. M. Moreno and P. Roca i Cabarrocas, EPJ Photovolt. **1**, 10301 (2010).
6. P. Vogt, P. De Padova, C. Quaresima, J. Avila, E. Frantzeskakis, M. C. Asensio, A. Resta, B. Ealet, and G. L. Lay, Phys. Rev. Lett. **108**, 155501 (2012).
7. D. Chiappe, C. Grazianetti, G. Tallarida, M. Fanciulli, and A. Molle, Adv. Mater. **24**, 5088 (2012).
8. A. Fleurence, R. Friedlein, T. Ozaki, H. Kawai, Y. Wang, and Y. Takamura, Phys. Rev. Lett. **108**, 245501 (2012).
9. L. Meng, Y. Wang, L. Zhang, S. Du, R. Wu, L. Li, Y. Zhang, G. Li, H. Zhou, W. A. Hofer, and M. J. Gao, Nano Lett. **13**, 685 (2013).
10. Y. Ding and Y. Wang, Nanoscale Res. Lett. **10**, 13 (2015).
11. A. Kara, H. Enriquez, A. P. Seitsonen, L. C. L. Y. Voon, S. Vizzini, B. Aufray, and H. Oughaddou, Surf. Sci. Rep. **67**, 1 (2012).
12. H. Nakano, Y. Sugiyama, T. Morishita, M. J. S. Spencer, I. K. Snook, Y. Kumai, and H. Okamoto, J. Mater. Chem. A **2**, 7588 (2014).

13. M. de Crescenzi, I. Berbezier, M. Scarselli, P. Castrucci, M. Abbarchi, A. Ronda, F. Jardali, J. Park, and H. Vach, ACS Nano **10**, 11163 (2016).
14. J. Zhao, H. Liu, Z. Yu, R. Quhe, S. Zhou, Y. Wang, C. C. Liu, H. Zhong, N. Han, J. Lu, Y. Yao, and K. Wu, Progr. Mater. Sci. **83**, 24 (2016).
15. A. E. Galashev, O. R. Rakhmanova, K. A. Ivanichkina, and A. S. Vorob'ev, Phys. Solid State **59**, 1242 (2017).
16. A. E. Galashev, O. R. Rakhmanova, and K. A. Ivanichkina, J. Struct. Chem. **59**, 877 (2018).
17. H. Q. Ho, Y. Honda, M. Motoyama, S. Hamamoto, T. Ishii, and E. Ishitsuka, Appl. Radiat Isot. **135**, 12 (2018).
18. M. L. Kozhukh, Nucl. Instrum. Methods Phys. Res., Sect. A **329**, 453 (1993).
19. I. S. Shlimak, Phys. Solid State **41**, 716 (1999).
20. J. M Soler, E. Artacho, J. D. Gale, A. García, J. Junquera, P. Ordejon, and D. Sanchez-Portal, J. Phys.: Condens. Matter **14**, 2745 (2002).
21. W. Hu, Z. Li, and J. Yang, J. Chem. Phys. **139**, 154704 (2013).
22. S. K. Gupta, H. R. Soni, and P. K. Jha, AIP Adv. **3**, 032117 (2013).
23. N. Pantha, A. Khaniya, and N. P. Adhikari, Int. J. Mod. Phys. B **29**, 1550143 (2015).
24. S. Xu, X. Fan, J. Liu, D. J. Singh, Q. Jiang, and W. Zheng, Phys. Chem. Chem. Phys. **20**, 8887 (2018).
25. T. Hussain, S. Chakraborty, and R. Ahuja, Chem. Phys. Chem. **14**, 3463 (2013).
26. M. A. Bin Hamid, C. K. Tim, Y. Bin Yaakob, and M. A. Bin Hazan, Mater. Res. Express **6** (5) (2019).
27. R. Zhou, L. C. L. Y. Voon, and Y. Zhuang, J. Appl. Phys. **114**, 093711 (2013).
28. J. E. Padilha and R. B. Pontes, J. Phys. Chem. C **119**, 3818 (2015).
29. J. Sivek, H. Sahin, B. Partoens, and F. M. Peeters, Phys. Rev. B **87**, 085444 (2013).
30. T. L. Brown, H. E. LeMay, and B. E. Bursten, J. Chem. Educat. **74** (4) (1997).
31. M. S. Silberberg, *Chemistry: The Molecular Nature of Matter and Change*, 5th ed. (McGraw-Hill, New York, 2009).
32. A. Y. Galashev and Yu. P. Zaikov, J. Appl. Electrochem. **49**, 1027 (2019).
33. W. Liu, H. Zhi, and X. Yu, Energy Storage Mater. **16**, 290 (2019).
34. A. E. Galashev, Yu. P. Zaikov, and R. G. Vladykin, Russ. J. Electrochem. **52**, 966 (2016).

Translated by E. Smorgonskaya